14th International Topical Meeting on Nuclear Reactor Thermal-Hydraulics, Operation and Safety (NUTHOS-14)
Vancouver, BC, Canada, August 25 – 28, 2024

# IAEA Benchmark CRP - I31038: Open Phase liquid-metal CFD results for fuel pin simulator

**Abdalla Batta, Andreas Class**
Karlsruher Institut für Technologie (KIT)
Hermann-von-Helmholtz-Platz 1,
76344 Eggenstein-Leopoldshafen Germany
abdalla.batta@kit.edu, class.andreas@kit.edu

## ABSTRACT

In the IAEA Coordinated Research Project "Benchmark of Transition from Forced to Natural Circulation Experiment with Heavy Liquid Metal Loop" (CRP - I31038) participants benchmark their simulation capabilities versus the experimental data obtained in the NACIE-Up facility (NAtural CIrculation Experiment-UPgrade) at ENEA (Italian National Agency for New Technologies, Energy and Sustainable Economic Development). The fuel pin simulator consists of 19 wire-wrapped pins. The liquid metal coolant first passes through an unheated cold section and then through an electrically heated section. In the heated section either all pins or only a fraction of the pins are heated to simulate power gradients in a nuclear reactor. During the experiments both the axial and the lateral temperatures are measured at suitable locations. Twelve results from different organizations contributed to the open phase benchmarking, where specifically the heating of all 19 pins, 9 pins and the 7 inner pins was studied. This will contribute to the validation and verification of the computational fluid dynamic tools for reactor design.
We have tried to deliver results that require minimal numerical resources, well-resolve all relevant geometric features and match the accuracy of the provided experimental data. In the second benchmark meeting at IAEA the results of the contributors were compared. It was confirmed that our modelling strategy leads to credible and accurate results at low numerical cost. In the paper we present details on the modelling approach and compare the numerical results to experimental data and preliminary CFD data resulting from all participants in the work package. Our simulation is ranked among the most reliable results.

**KEYWORDS**

Liquid-metal, Wire-wrap, Fuel assembly, CFD, Benchmark

## 1.0 INTRODUCTION

In this study, open phase liquid metal CFD results for forced and natural convection bundle flow are compared to experimentally offered data by IAEA Benchmark CRP - I31038. The benchmark study aims at obtaining confidence in simulation capabilities for liquid metal flow when large thermal loads occur. Details on the benchmark specification and background are given in [1]. In 2017 the experimental campaign was performed with the NACIE-UP (NAtural CIrculation Experiment- UPgraded) facility. The benchmark was proposed by ENEA Brasimone Research Centre (Italy). The benchmark exercise allows stand-alone system codes, coupled CFD/TH system codes and stand-alone CFD simulations. Lead Bismuth Eutectic (LBE) is used as coolant so that the study is relevant for liquid-metal cooled fast reactors. The NACIE-UP facility consists of a rectangular loop. Fig. 1 shows the CAD drawing of the test section. Indicated is the origin of the used coordinate system. In the figure the gravity direction is indicated by an arrow, i.e. the flow direction is pointing upward in the real world. The loop pipes have an inner diameter of 62,68mm. The test section is located at the lower end of the vertical extent, where the riser section is not depicted. Flow enters the test section from the lower loop horizontal pipe. The heated section is placed above a preconditioner section and begins at z=0 as shown in figure 1. The flow in the experiment is driven by forced or natural convection. For the forced-convection cases a gas-lift pumping technique is applied, see [1] for more details.

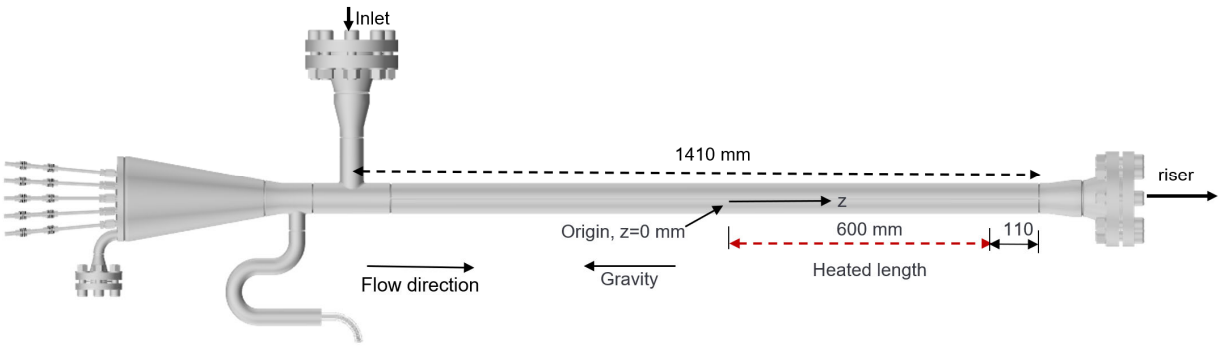


**Figure 1: CAD drawing of the test section and origin of the used coordinate system [1].**

The fuel pin simulator (FPS) consists of 19 wire wrapped pins. Heating of pins can be activated individually to achieve various heating configurations. The installed heating power of all pins is identical. A maximum power of 250 kW can be obtained when all pins are heated. The active heated length of the pins is 600 mm. The pin diameter is 6.55 mm. This results in a maximum wall heat flux near 1 MW/m$^2$. The complete loop including the test section are insulated to achieve an adiabatic experimental condition. The benchmark has an open and a blind phase. In the open phase of the benchmark, two symmetric heating configurations are studied. In the blind phase asymmetric heating is considered. Figure 2 shows a cross section in the considered cases. The red color indicates the activated heater in each test. The cases ADP10, ADP 06 are considered for the open phase, while case ADP07 is considered in the blind phase. The open phase benchmark results are used to select suitable models and computational parameters. These are applied in the blind phase for the more complex situation of asymmetrical heating. The pins are arranged in a hexagonal lattice (central, middle, and outer rank). The triangular pitch of the FPS is 8.4 mm, as the wire diameter is 1.75 mm. The pitch to diameter ratio equates to 1.2824. This corresponds to a hydraulic diameter of 3.84 mm. The wires are twisted helically around the pins as horizontal spacers. The sweep direction is counterclockwise with a streamwise pitch of 262 mm.

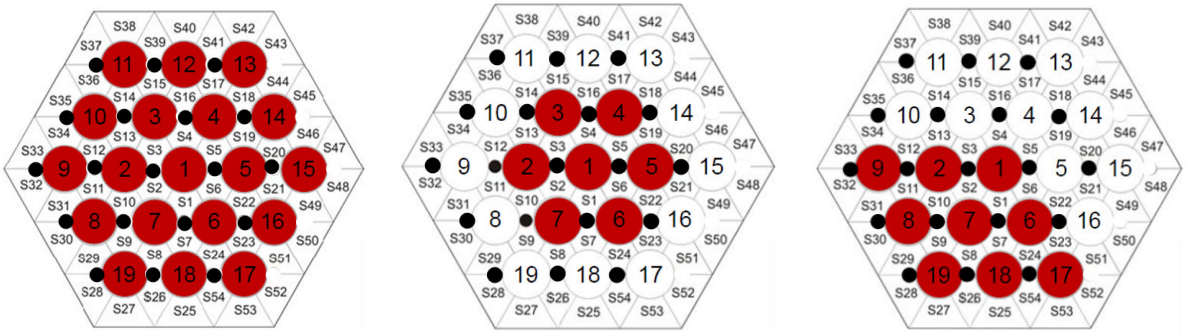


**Figure 2: Bundle cross section; benchmark test cases ADP10, ADP06 and ADP07; active pins (in red) during test, [2].**

In this article, results obtained for case ADP06 are presented. A suitable numerical setup (including boundary conditions, mesh, and domain) obtained in the previous study of case ADP10 are applied in the new computations of case ADP06. The previous results for case ADP10 are published in [2]. The test case ADP10 corresponds to the heating of all pins. In the case ADP06 the central and the second inner row are heated, while the outer rank remains unheated. Note, each studied case consist of two steady states results and a transient case. Here we restrict ourselves to the steady state cases.

In case of forced convection, the gas-lift pump is activated resulting in the steady state 1. Stopping the pumping results in an intermediate transient and subsequently in the steady state 2. Here natural convection is driven by the buoyancy resulting from the heated pins.

Figure 3a shows the position of the measurement sections A, B and C. The position and the numbering of the thermocouples (TC) in the three planes are listed in figure 3b. For pin 3 an array of 13 thermocouples (55 to 67) is installed to measure the axial wall temperature. Those thermocouples measuring wall temperature are indicated with red dots while the green dots denote the thermocouples in the bulk fluid.

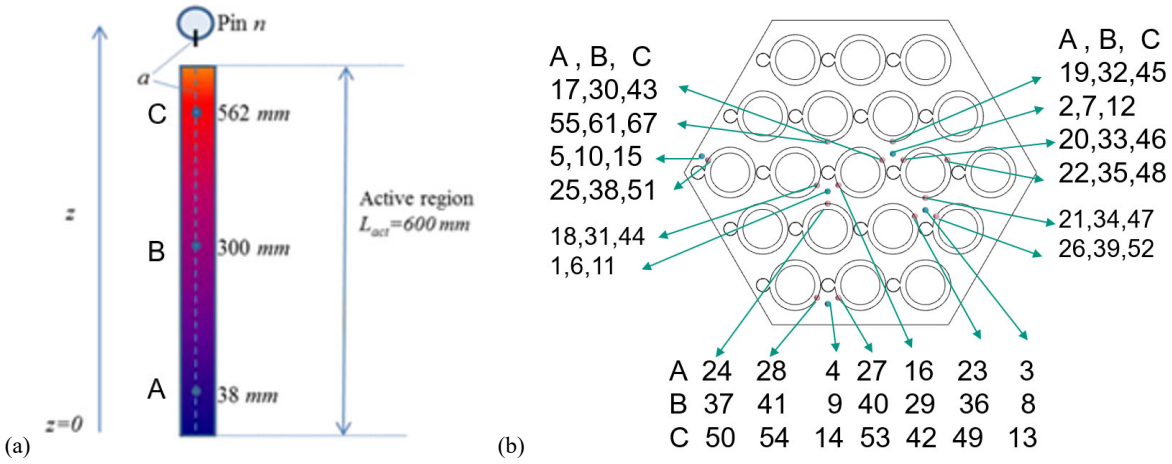


**Figure 3: (a) Location of planes for TC measurements in the test section (A at 38mm, B at 300mm and C at 562mm) (b) location and names of thermocouples in measurements planes [2].**

## 2.0 BENCHMARK SPECIFICATION FOR CASE ADP06

In this section we will provide a short summary of the essential benchmark specifications. The reader is referred to [1] for more details. For case ADP06, table 1 contains the integral operational conditions of the steady states 1 and 2, corresponding to forced and natural convection, respectively.

**Table 1 Integral parameters of the test ADP06 [1]**

| | **Steady state 1** | | | **Steady state 2** | | |
|---|---|---|---|---|---|---|
| **Parameter** | **Data** | **$\sigma$** | **$\sigma$[%]** | **Data** | **$\sigma$** | **$\sigma$[%]** |
| $\dot{m}_{gas}[Nl/min]$ | 10 | 0.5 | 5 | 0 | 0 | 0 |
| $\dot{m}_{LBE}[kg/s]$ | 2.66 | 0.29 | 11 | 1.33 | 0.14 | 11 |
| $T_{IN,FPS}$[°C] | 234.5 | 1.5 | | 221.2 | 1.5 | |
| $\Delta T_{FPS}$[°C] | 68.4 | 0.8 | 1.1 | 130.1 | 0.5 | 0.4 |
| $Q_{nom}$ [w] | 30000 | 50 | 0.2 | 30000 | 51 | 0.2 |
| $Q_{eff}$ [w] | 26800 | 1052 | 3.9 | 25400 | 952 | 3.7 |
| $Q_{pre}$ [w] | 2508 | 438 | 17.5 | 2675 | 230 | 8.6 |
| $Q_{tfm}$ [w] | 1933 | 3 | 0.2 | 1652 | 4 | 0.3 |

The table lists error estimates for various integral parameters. As forced and natural convection is driven by buoyancy, the LBE mass flow shows a quiet large uncertainty equating to 11%. Note, that the electric current axially passes along the full length of the pins. Even though heating predominantly occurs in the heated

section a smaller part is generated in the preconditioning section. Both the effective heating in the heated section $Q_{eff}$ and the $Q_{pre}$ in the preconditioning will be considered in the simulations. An additional heating $Q_{tfm}$ is the power supplied to a thermal flow meter installed upstream of the test section. $Q_{tfm}$ is not considered in the simulation. A requirement of the benchmark was, that all participants ensure that the average inlet temperature to the heated section ($T_{in,FPS}$) is identical for all. This specified FPS inlet temperature at z=0mm is tabulated in table 1.

Data for physical properties of LBE is selected according to the OECD handbook [3]. The fuel pin simulators are made of multiple layers of different materials. The outer layer is stainless-steel cladding (AISI316L with physical properties in [4]). The second layer is an electrical insulating Bohrium Nitride (BNi) with physical properties from [5]. A very thin Inconel600 layer with assumed steel properties is placed in the BNi-layer. At the pin center an inner copper rod is separated from the Inconel600 layer by electrically insulating Bohrium Nitride.

## 3.0 NUMERICAL MODEL AND RESULTS

The model used for simulation of benchmark cases is based on previous experiences gained at KIT, see [2,6-9]. As mentioned above the validated and verified model used for the simulation of case ADP10 reported in [2] will be applied here. A summary of case ADP10 specifications are given in table 2.

**Table 2 Integral parameters of the test ADP10. [2]**

| | **Steady state 1** | | | **Steady state 2** | | |
|---|---|---|---|---|---|---|
| **Parameter** | **Data** | $\boldsymbol{\sigma}$ | $\boldsymbol{\sigma}$**[%]** | **Data** | $\boldsymbol{\sigma}$ | $\boldsymbol{\sigma}$**[%]** |
| $\dot{m}_{gas}[Nl/min]$ | 10 | 0.5 | 5 | 0 | 0 | 0 |
| $\dot{m}_{LBE}[kg/s]$ | 2.56 | 0.28 | 11 | 1.31 | 0.14 | 11 |
| $T_{IN,FPS}$[°C] | 231.3 | 1.5 | | 219.5 | 1.5 | |
| $\Delta_{TFPS}$[°C] | 72.0 | 0.7 | 0.9 | 140.6 | 0.3 | 0.2 |
| $Q_{nom}$ [w] | 30000 | 50 | 0.2 | 30000 | 44 | 0.1 |
| $Q_{eff}$ [w] | 27000 | 1053 | 3.9 | 27000 | 1010 | 3.7 |
| $Q_{pre}$ [w] | 2236 | 403 | 18 | 2339 | 217 | 9.3 |
| $Q_{tfm}$ [w] | 1915 | 3 | 0.2 | 1644 | 4 | 0.3 |

In [2] two different representations of the heater were considered. Tests of various heater models showed small influence on results. Additionally, two meshes were compared. A small sensitivity of results with respect to the compared meshes was found. The fluid domain and the tested heaters are shown in figure 4a It also depicts the used computational domain. It illustrates the extent of the fluid domain and the considered details of the heater and wrapper. At the outer boundary of the wrapper an adiabatic condition is assumed.

Considering modelling of the heater, in a first trial, a uniform heat flux was applied on the inside of the cladding (short heater, marked red in figure 4a). The other pin layers were excluded from the simulation and the heat in the preconditioning part was ignored. In the second trail, a detailed simulation of all layers of the heater are considered. Heat was uniformly generated in the Inconel layer. Both the heat generation in the heated and preheated section of each pin was considered. In both trials the given $T_{IN,FPS}$ in the specification was reserved. For the short heater simulation (trial 1) the mesh is composed of 49 M (Million)

fluid cells and 13 M solid cells (mesh I). The mesh for the long heater case (trial 2) uses 96 M fluid cells and 29 M solid cells for the heater and wrapper (mesh II). Figure 4b shows a cross section of the mesh II used in the simulation. The SST turbulence model with all y+ wall treatment is selected for the simulation of all benchmark cases. The Star CCM+ CFD commercial code is used. Both studies of short and long heater with mesh I and II show a reliable agreement with experiment result. However, the simulation considering details of the heater, i.e. mesh II, had shown slightly better agreement. (see [2] for more details). Buoyancy induced by gravity was considered in all the calculations. Preliminary benchmark results rank our simulation for case ADP10 as the best considering the average error compared to other partners.

For the study of case ADP06, we use the validated and verified CFD model based on mesh II with detailed heater. Figure 4c shows the resulting Y+ values for the steady state case 2. The range of Y+ values are suitable for SST and the applied wall function treatment.

Selected results representing velocity and temperature fields for the natural convection case (ADP06 case steady state2) are presented and discussed below. Figure 5a and b depict tangential (i.e. lateral or secondary) and axial velocity contours at section A, respectively. Strong mixing induced by the wire-wraps can be seen from the magnitude of resulting secondary and axial normal velocity. Preliminary benchmark evaluation indicates that the maximum tangential velocity in plane A may be influenced by the applied inlet condition. In our study we applied a simple uniform inlet condition, while the real condition at this location is still weakly influenced by the upstream geometric configuration. The preliminary evaluation of the benchmark results of distinct handling of the inlet boundary could result in slightly lower maximum secondary flow velocities, around 10% less compared to figure 5a.

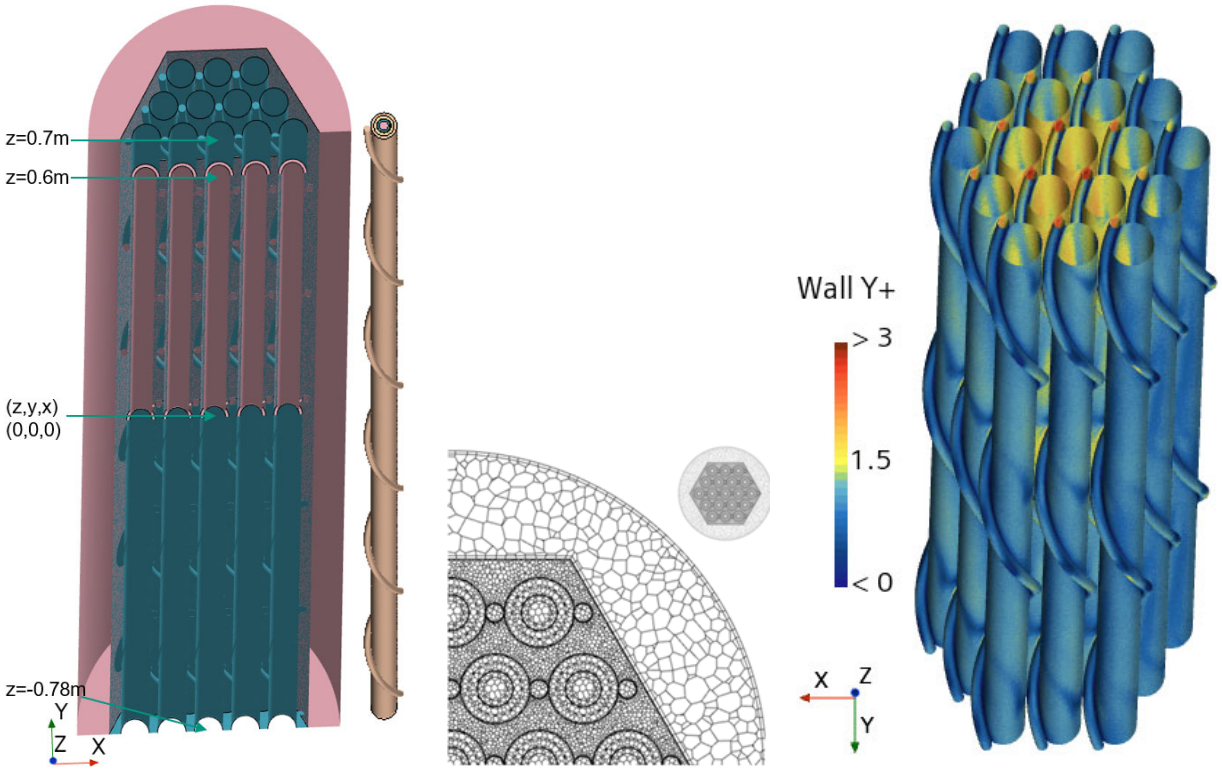


**Figure 4: a) Computational domain with short, simplified heater (left) and detailed simulated long heater (right). b) Cross section of meshes used in simulation. c) Y+ values, ADP06 case steady state2.**

Figure 6 shows the temperature contours of case ADP06, steady state2, where the flow is driven by natural convection. Even though the outer rank of pins is unheated, at some locations within this region, high temperatures occur due to the strong mixing effect of the wire-wraps. Comparisons of simulated versus measured local temperature data are shown as a bar chart in Figure 7 and 8. The two figures correspond to

the forced and natural convection cases, respectively. The experimental data has been published and discussed in [10-12]. Simulations show very good agreement compared to the experimental data in most positions. Throughout all positions, the absolute difference of compared temperatures is small and quiet uniformly distributed. Therefore, in regions with high temperatures the relative errors become small. Conversely, at positions with low temperature (in particular at section A close to the inlet), when computing relative errors, the relative error shows higher numbers since the reference temperature difference in the denominator (experimental data) is small. Moreover, in the regions of small temperature increase (far from bundle centre) the comparison between experimental results and numerically computed temperature shows higher uncertainty than in regions with higher temperature increase (near centre of the bundle). The uncertainties can be attributed to many factors. Note, that the sensitivity of used TC is near ±1.5°C for the considered temperature range. Moreover, the results are interpreted using an averaged FPS inlet temperature and a bulk temperature. These derived integral experimental values are based on limited measured values and weighting factors (see [1]). These may introduce additional uncertainty. Finally, other sources of uncertainty can be related to the assumed uniform inlet profile in the simulation (discussed above), material properties, the capability of the applied CFD model, etc.

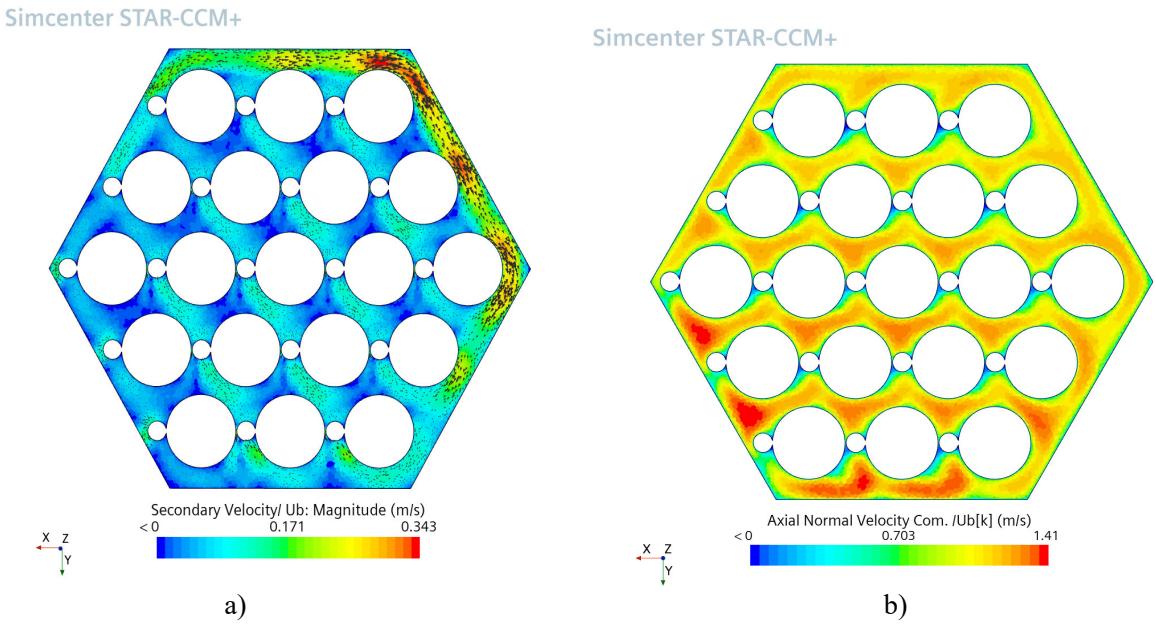


**Figure 5: Velocity contours at section A, case ADP06 case steady state2,**

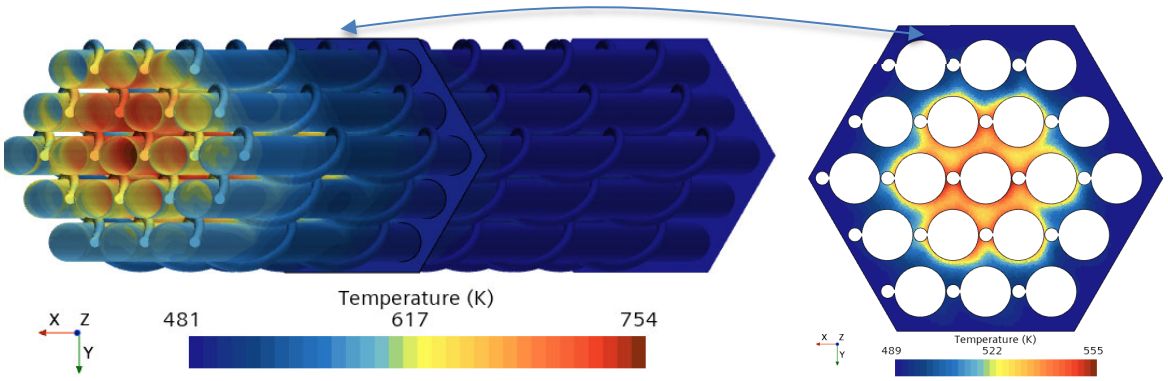


**Figure 6: Temperature contours for natural circulation results, mesh II with long heater, case ADP06 case steady state 2.**

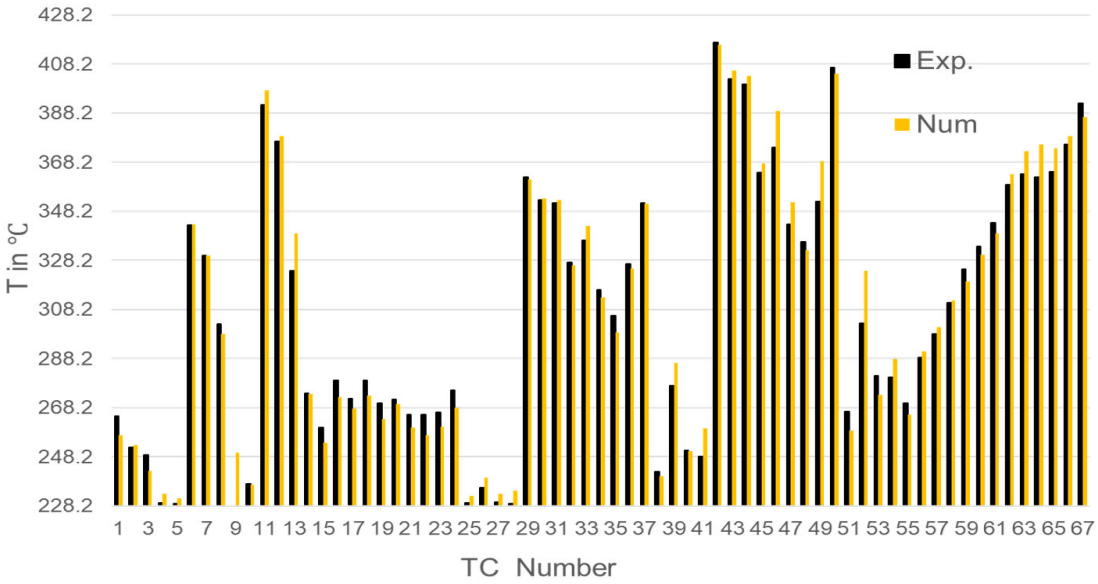


**Figure7: Forced convection results, mesh II with long heater, case ADP06 case steady state1.**

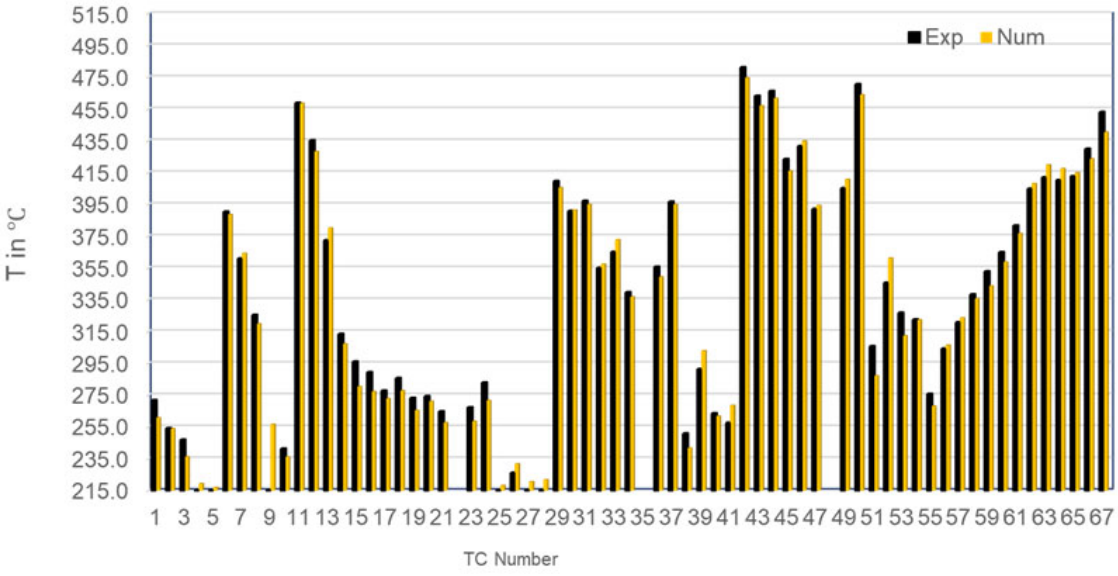


**Figure 8: Natural convection results, mesh II with long heater, case ADP06 case steady state2**

A preliminary benchmark evaluation using data of partners was presented in the last benchmark meeting. A final CRP report which compares results of all participating organizations will soon be published. In the preliminary benchmarking of the four open phase cases 12 results are analysed considering the average error. Three thermocouples TC9, TC22, TC35 and TC48 are not considered in the benchmark evaluation. The preliminary evaluation shows that our selected CFD parameters results is one of the most accurate and best ranked simulations carried out by benchmark participants. The difference between our results and yet better ranked results is minimal. It is noticed that the average error of case ADP10 was slightly lower than for case ADP06. We attribute differences to the heat transfer in the lateral direction. For case ADP10 the heat transfer in the axial direction is dominant. For case ADP06 the radial direction becomes more important since the outer rank of pins is not heated. This with flow mixing due to wires enhance the heat transfer in the lateral direction significantly. Another factor could be related to the applied uniform inlet condition. We noticed that in the natural convection case ADP06 the lateral velocity shows pronounced peak values at the outer rank of pins in section A, see top right region in figure 5a. These values are sensitive to the inlet conditions. Consequently, lateral heat transfer is more sensitive for case ADP06. Downstream of the inlet

mixing within the rod bundle reduces uncertainty. In measurement plane A (just downstream of FPS inlet) the relative error between experimental and numerically calculated temperature is larger than in sections B and C.

## 4.0 CONCLUSIONS

We participated in the CRP NACIE -UP benchmark and applied our long experience in CFD simulations on rod bundle thermohydraulic. As expected, we were able to deliver good results with effectively balanced accuracy and numerical effort. We used the Star-CCM+ code the SST turbulence model and all Y+ wall treatment and a mesh that was tested in an open phase case of the benchmark.

Our results show deviations relative to the measured data that are of similar order of magnitude as the uncertainty of the measurements, material properties and geometrical dimensions. No systematic trends in these deviations could be found. However, relative errors using the temperature variation in a cross section as their reference, show large values in the inlet section where the temperature is almost uniform. Overall, our simulation results indicate that the chosen modelling strategy takes account of the relevant physics with sufficient accuracy throughout the bundle.

In conclusion, the applied methodology has now successfully passed its validation and verification, so that it will be used without modification for the blind phase case ADP07 of the benchmark.

## 5.0 ACKNOWLEDGMENTS

This work has been supported by the Framatome Professional School at KIT. The data and information presented in the paper are part of an ongoing IAEA coordinated research project on "Benchmark of Transition from Forced to Natural Circulation Experiment with Heavy Liquid Metal Loop – CRP-I31038. The work presented is original but some or all of the information may need to be included in a book publication at a later date as part of the output of the International Atomic Energy Agency coordinated research project on "Benchmark of Transition from Forced to Natural Circulation Experiment with Heavy Liquid Metal Loop – CRP-I31038.

## 6.0 REFERENCES

[1] Di Piazza, H. Hassan, P. Lorusso, D. Martelli, “Benchmark specifications for nacie-up facility: non-uniform power distribution tests”, Ref. NA-I-R-542, Issued: 28/02/2023 ENEA, Italy.
[2] Batta, A. Class A., “CFD Validation Of Forced And Natural Convection For The Open Phase Of IAEA Benchmark CRP - I31038”, SCOPE (Saudi International Conference On Nuclear Power Engineering) 13–15 Nov 2023 King Fahd Conference Center, KFUPM, Dhahran, KSA
[3] N. E. Agency, “Handbook on Lead-bismuth Eutectic Alloy and Lead Properties, Materials Compatibility, Thermal-hydraulics and Technologies,” *Nucl. Sci.*, pp. 647–730, 2015.
[4] C.S.Kim, “Thermophysical properties of stainless steels”, ANL-75-55, 1975.
[5] Thermocoax, private communication
[6] Batta, A. Class, “CFD validation for partially blocked wire-wrapped liquid-metal cooled 19-pin hexagonal rod bundle carried out at KIT-KALLA”, Proc. of the 19th International Topical Meeting on Nuclear Reactor Thermal Hydraulics (NURETH-19) Log nr.: 36240 Brussels, Belgium, March 6 - 11, 2022
[7] Batta, A. Class, A. Pacio, J. Vlidation for CFD thermalhydraulic simulation for liquid metal cooled blocked 19-pin hexagonal wire wrapped rod bundle experiment carried out at KIT-KALLA, AMNT 50, 2019
[8] Batta, A.: Class, A. Thermalhydraulic CFD validation for liquid metal cooled 19-pin hexagonal wire wrapped rod bundle, paper 28473, Nureth 18.
[9] Batta, A.: Class, A.; Pacio, J. Numerical analysis of a LBE-cooled blocked 19-pin hexagonal wire wrapped rod bundle experiment carried out at KIT-KALLA within EC-FP7 project MAXSIMA” Paper ID 20532, Nureth 17,
[10] R. Marinari, I. Di Piazza, M. Angelucci, D. Martelli, “POST-TEST CFD ANALYSIS OF non-uniformly heated 19-pin fuel bundle cooled by HLM”, ICONE26-81307, Proc. ICONE26, July 22-26, 2018, London.
[11] M.Angelucci, I. Di Piazza, M.Tarantino, R. Marinari, G. Polazzi, V. Sermenghi, “Experimental tests with non-uniformly heated 19-pins fuel bundle cooled by hlm”, ICONE26-81216, Proc. ICONE26, July 22-26, 2018, London.
[12] R. Marinari, I. Di Piazza, M. Tarantino, M. Angelucci, D. Martelli, “Experimental tests and post-test analysis of non-uniformly heated 19-pins fuel bundle cooled by Heavy Liquid Metal”, Nucl.Eng. Des., Vol. 343, pg. 166-177, 2019.